

# Improvement of Himawari-8 observation data quality

3 July 2017

Meteorological Satellite Center  
Japan Meteorological Agency

The Japan Meteorological Agency (JMA) plans to modify its Himawari-8 ground processing system at 04:00 UTC on 25 July 2017 in order to improve the quality of Himawari-8 imagery and to update the Himawari Standard Data (HSD) format with the latest calibration coefficients in consideration of sensor sensitivity. The modification will include:

- 1) Reduction of banding and stripe noise
- 2) Improvement of quantization noise
- 3) Updating of the HSD format

## 1) Reduction of banding and stripe noise

Current Himawari-8/Advanced Himawari Imager (AHI-8) imagery from the visible and near-infrared (VNIR) bands (i.e., Bands 1 to 6) includes banding and stripe noise in the east-west direction (Figs. 1 (a) and 2 (a)). These are generally attributable to incorrect calibration slopes derived from solar diffuser (SD) observation by the Himawari-8 satellite. Specifically in this regard, the bidirectional reflectance distribution function (BRDF) of the AHI-8 SD underwent an erroneous reversion from north to south during calibration slope derivation.

In relation to AHI-8 VNIR imagery, calibration coefficients for Bands 1 to 6 will be corrected at 04:00 UTC on 25 July 2017. The new calibration slopes are expected to significantly reduce banding (Fig. 1 (b)) and striping (Fig. 2 (b)).

The new slopes will be determined by averaging solar diffuser observation data collected from 7 March to 22 May 2015. As the same SD observation dataset will continue to be used after the updates, any changes

in AHI-8 characteristics, such as sensitivity degradation, will not be taken into account in the updated slopes.

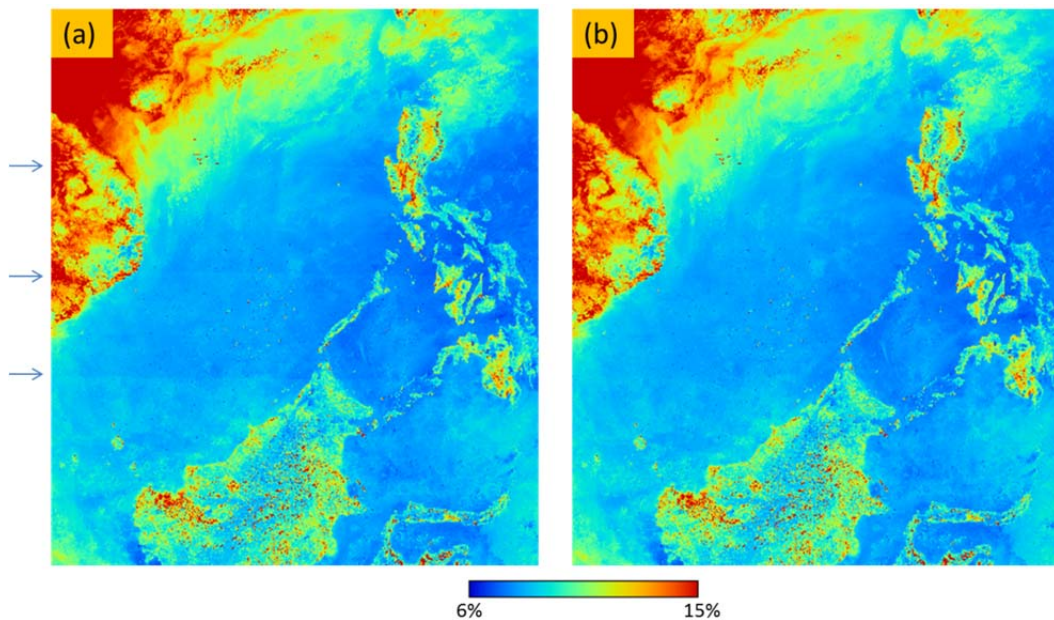


**Fig. 1** (a) Minimum albedos<sup>1</sup> [%] of AHI-8 Band 2 as extracted from 22 HSDs for 03:10 UTC from 10 to 31 March 2016. (b) As per (a), but with bug-fixed calibration slope computation. The extraction is performed at each HSD pixel for (a) and (b). The three clear lines observed at swath boundaries (i.e., banding) in (a) are significantly reduced in (b).

---

<sup>1</sup>  $A = \pi I / S_0$

$A$ : albedo;  $I$ : radiance [ $\text{W} / (\text{m}^2 \text{sr} \mu\text{m})$ ];  $S_0$ : band solar irradiance [ $\text{W} / (\text{m}^2 \mu\text{m})$ ]

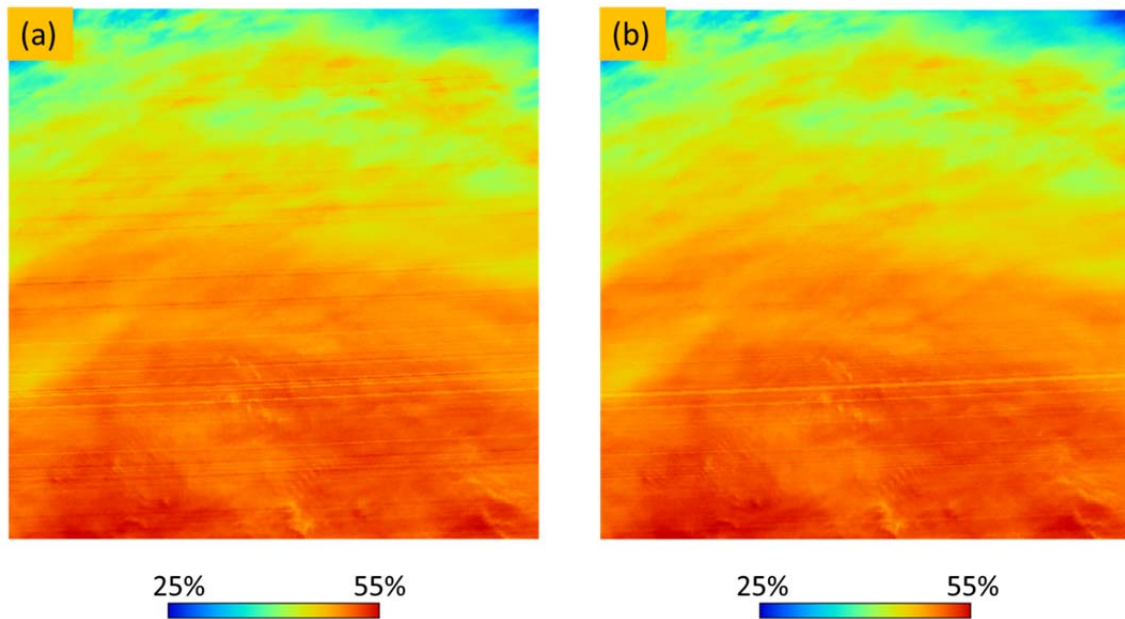


**Fig. 2.** (a) Albedos [%] of AHI-8 Band 2 at 03:10 UTC on 15 March 2016. (b) As per (a), but with bug-fixed calibration slope computation. The clear striping seen in (a) is mitigated in (b).

## 2) Improvement of quantization noise

AHI-8 earth observation samples are downlinked to the ground station by truncating digital counts from 14 bits to 11 bits (Bands 1, 2, 3, 4, 5, 6, 8, 9, 16) or 12 bits (Bands 10, 11, 12, 13, 14, 15) except for Band 7. No truncation is applied to other information such as black body observation data for infrared calibration. To compensate biases stemming from such truncation, a value of 0.5 was previously added to the raw digital counts for all AHI-8 bands during HSD generation.

However, as this practice was found to cause quantization noise, the values added to raw digital counts are now:

Bands 1, 2, 3, 4, 5, 6, 8, 9, 16: +0.4375

Bands 10, 11, 12, 13, 14, 15: +0.375

Band 7: 0

Table 1 shows how the correction of raw digital counts affects albedo in VNIR bands, and Table 2 shows related effects on brightness temperature in other infrared bands (Table 2; averaging for the full-disk area as of 12:10 UTC on 4 October 2016).

**Table 1** Impacts of raw digital count correction on albedo [%] in VNIR bands

| band | bits | corrected raw digital counts | change in albedo (%) |
|------|------|------------------------------|----------------------|
| B01  | 11   | -0.0625                      | -4.9E-03             |
| B02  | 11   | -0.0625                      | -5.0E-03             |
| B03  | 11   | -0.0625                      | -6.8E-03             |
| B04  | 11   | -0.0625                      | -8.4E-03             |
| B05  | 11   | -0.0625                      | -4.5E-03             |
| B06  | 11   | -0.0625                      | -5.2E-03             |

**Table 2** Impacts of raw digital count correction on brightness temperature [K] in IR bands

| band | bits | corrected raw digital counts | change in brightness temperature (K) |
|------|------|------------------------------|--------------------------------------|
| B07  | 14   | -0.5000                      | -0.129                               |
| B08  | 11   | -0.0625                      | -0.015                               |
| B09  | 11   | -0.0625                      | -0.012                               |
| B10  | 12   | -0.1250                      | -0.011                               |
| B11  | 12   | -0.1250                      | -0.009                               |
| B12  | 12   | -0.1250                      | -0.008                               |
| B13  | 12   | -0.1250                      | +0.009                               |
| B14  | 12   | -0.1250                      | +0.008                               |
| B15  | 12   | -0.1250                      | +0.011                               |
| B16  | 11   | -0.0625                      | +0.022                               |

### 3) Updating of the HSD format

Sensitivity and other sensor performance characteristics determined in pre-launch ground testing may change in orbit. Figure 3 shows sensitivity trends of AHI-8 VNIR bands with an SD on board the Himawari-8 satellite as a solar calibration target. The validation results indicate degradation of approximately 0.5% a year in Bands 1 to 4.

Calibration slopes determined at the pre-launch stage were used provisionally after launch, and the coefficients were updated on 8 June 2015 using SD observation data. AHI-8 SD observation is performed approximately every two weeks. The calibration slopes derived from 7 SD observation events from March to May 2015 were averaged and used for the update. No further updates have been implemented.

At 04:00 UTC on 25 July 2017, JMA will update part of the Header block in Himawari Standard Data format to incorporate the latest calibration

information derived from SD observations for VNIR bands. Figure 4 summarizes the update. Among the 104 bytes spare in the #5 calibration information block, 24 were assigned to 1) updating the time (MJD; modified Julian date) of the latest calibration coefficients; 2) the latest slope for the count-radiance conversion equation, and 3) the latest intercept for the count-radiance conversion equation. Based on 2) and 3), users can derive radiances in which the sensor trend is appropriately considered. JMA plans to update its calibration information periodically, and only the latest such information will be stored as the most recent. A history of calibration information is available on the Meteorological Satellite Center's webpage.

The calibration information (i.e., the value of Nos. 8 and 9 in the #5 calibration information block) used will still be that derived from SD observations conducted between March and May 2015. Accordingly, this format update does not affect users' current processing.

The format for IR bands will not change.

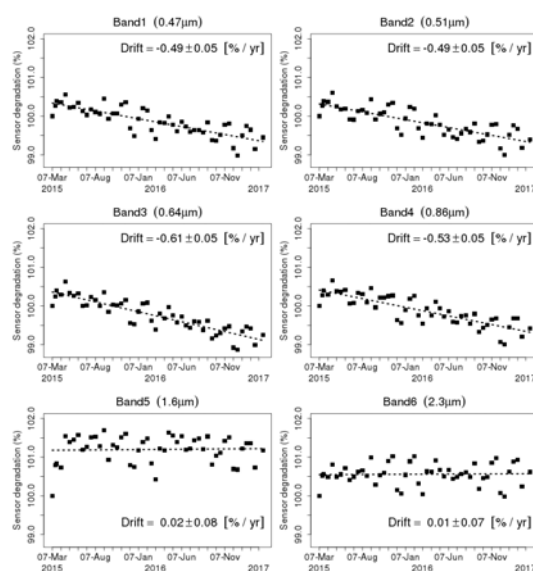


**Fig. 3** Sensor sensitivity trends for AH1-8 VNIR bands

Time-series representations for the inverse of calibration slopes derived from AH1-8 SD observations. Averaged values over for detectors and values normalized for the first observation on 7 March 2015 are shown.

| Visible, near-infrared band (Band No. 1 – 6)    |  |    |     |   |  |
|---|--|----|-----|---|--|
| (Band No. 1: backup operation (See Table 4 bb)) |  |    |     |   |  |
| 10  | Coefficient (c') for transformation from radiance (I) to albedo (A) <sup>6</sup> | R8 | 8   | 1 | $A = c' I$<br>A [1]<br>$c' [(m^2 sr \mu m) / W]$<br>$I [W / (m^2 sr \mu m)]$ |
| 11  | Spare  | —  | 104 | 1 | Spare  |

↓

| Visible, near-infrared band (Band No. 1 – 6)    |  |    |    |   |   |
|---|--|----|----|---|---|
| (Band No. 1: backup operation (See Table 4 bb)) |  |    |    |   |   |
| 10  | Coefficient (c') for transformation from radiance (I) to albedo (A) <sup>6</sup>                             | R8 | 8  | 1 | $A = c' I$<br>A [1]<br>$c' [(m^2 sr \mu m) / W]$<br>$I [W / (m^2 sr \mu m)]$  |
| 11  | Updated time of latest calibration coefficients in the following No. 12 and No. 13                           | R8 | 8  | 1 | [MJD]   |
| 12  | Calibration coefficient (Slope) for correcting sensor's sensitivity change (updated No. 8 of this block)     | R8 | 8  | 1 | Radiance =<br>Slope x Count + Intercept<br>Radiance [W / (m <sup>2</sup> sr μm)]  |
| 13  | Calibration coefficient (Intercept) for correcting sensor's sensitivity change (updated No. 9 of this block) | R8 | 8  | 1 | Slope [W / (m <sup>2</sup> sr μm count)]<br>Intercept [W / (m <sup>2</sup> sr μm)]<br>Count (See Block #12 1 count value of each pixel) |
| 14  | Spare  | —  | 80 | 1 | Spare   |

**Fig. 4** Himawari Standard Data format update